Journal of Sound and Vibration (1997) **208**(5), 745–761

A MULTIPLE HARMONIC BALANCE METHOD FOR THE INTERNAL RESONANT VIBRATION OF A NON-LINEAR JEFFCOTT ROTOR

Y. B. KIM

Department of Mechanical Engineering, Chonnam National University, Kwangju, Republic of Korea

AND

S.-K. CHOI

Rotating Machinery Group, Korea Institute of Machinery & Materials, Taejon, Republic of Korea

(*Received* 12 *June* 1996, *and in final form* 8 *July* 1997)

A multiple harmonic balance method is presented in this paper for obtaining the internal resonant steady state vibration of a Jeffcott rotor with a piecewise-linear non-linearity at the bearing support. The method utilizes the *hypertime* concept, which isolates each frequency component of a response into pseudo-time domains. Explicit Jacobians are derived to obtain stable convergence solutions in the iteration process. The frequency components of the non-linear restoring force part are analytically expressed from those of the displacement part, using the Galerkin technique to guarantee a convergent solution. As the method utilizes general and systematic computational procedures, it can be applied to analyze the multi-tone or combination-tone responses for higher-dimensional non-linear systems such as multi-disk rotors or automotive drivelines with multiple excitational inputs. To demonstrate the accuracy and effectiveness of the proposed method, various simulation results are studied and the results of multiple HBM are compared with those from numerical integration.

1. INTRODUCTION

It is well known that the harmonic balance method (HBM) is one of the most commonly used approaches for analyzing strong non-linear dynamical systems [1, 2]. Although HBM requires the prior determination of the retained harmonic terms and involves elaborate algebraic formulation, it has been successfully applied to the analysis of the responses of various non-linear systems in several engineering fields.

Nevertheless, the application of the aforementioned method is limited to predicting periodic vibrations only, whereas, in reality, many engineers and researchers often encounter problems of analyzing and designing the vibration of self-excited aperiodic rotor systems or dual rotor systems in aircraft gas turbines, or analyzing non-linear dynamical systems subjected to multi-frequency excitations, such as the ALP (articulated loading platform) in structural engineering, or designing communication circuits such as modulators and mixers in electrical engineering.

0022–460X/97/500745 + 17 $25.00/0/sv971221

During the past decade, several attempts have been made to devise methods for obtaining steady state, aperiodic or internal resonant responses of systems under single- or multi-excitation frequencies. The methods developed so far may be classified into three categories: (1) a frequency domain approach [3, 4]; (2) a time domain approach [5–8]; and (3) a hybrid approach in which time and frequency domains are alternatively utilized [9].

Lau *et al*. [3] developed the incremental harmonic balance method in obtaining the steady state aperiodic solutions in a clamped–hinged beam, in which they utilized a multiple integration formula by applying the Galerkin procedure. Their method could provide each frequency component involved in the system response, and it requires an approximate solution form where the incremental step starts. Ushida and Chua [4] presented a frequency domain approach based on a generalized harmonic balance method (GHBM) with alternating discrete and inverse discrete Fourier transform techniques for the analysis of non-linear systems with two excitation frequencies. They used equally spaced time intervals to obtain a discrete Fourier transform matrix for an almost periodic signal. As they used a least squares approximation to obtain the inverse discrete Fourier coefficients, ill-conditioning problems might occur unless a more elaborate and lengthy numerical scheme is utilized as mentioned by Kundert [4]. A fixed point algorithm (FPA), a shooting-type method for almost periodic solutions of a system with multi-inputs, was introduced by Kaas-Peterson [5, 6]. Kaas-Peterson reformulated the problem of finding aperiodic solutions of a system with two forcing frequencies as a fixed point problem in the redefined Poincaré mapping. An interpolation process is utilized to obtain a fixed point in the Poincaré space. Ling [7] presented a modified version of FPA method by introducing the Jacobian matrix using analytical derivatives instead of numerical differentiation. The FPA, however, has a drawback in its use of an interpolation technique to locate the fixed point in the Poincaré map. It requires very careful selection of the Poincaré points and the interpolation scheme. Moreover, the selection schemes might differ if other systems are involved (see reference [8]).

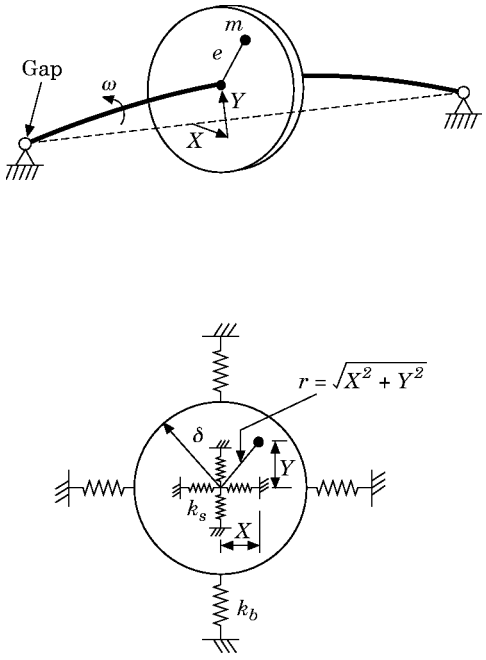

Figure 1. A Jeffcott rotor model with bearing clearances.

TABLE 1

Frequency component comparison ($\Omega = 2{\cdot}0$, $\alpha = 1{\cdot}0$, $\zeta = 0{\cdot}2$, $\gamma = 0{\cdot}3$)

Frequency component	Double HBM	FFT
DC component for x	8·255811	8·255395
DC component for y	−27·521273	−27·520680
ω_1	1·2987677	1·299063
$2\omega_1$	$4{\cdot}3728 \times 10^{-5}$	$4{\cdot}0785 \times 10^{-5}$
$3\omega_1$	$1{\cdot}3586 \times 10^{-5}$	$2{\cdot}2445 \times 10^{-5}$

TABLE 2

Frequency component comparison ($\Omega = 2{\cdot}3$, $\alpha = 5{\cdot}0$, $\zeta = 0{\cdot}2$, $\gamma = 0{\cdot}3$)

Frequency component	Double HBM	FFT
DC component for x	12·940489	12·940490
DC component for y	−22·585759	−22·585760
ω_1	1·0913874	1·091388
$2\omega_1$	$2{\cdot}1235 \times 10^{-5}$	$1{\cdot}4324 \times 10^{-5}$
$3\omega_1$	$0{\cdot}8745 \times 10^{-5}$	$0{\cdot}3133 \times 10^{-5}$

TABLE 3

Frequency component comparison ($\Omega = 3{\cdot}0$, $\alpha = 1{\cdot}0$, $\zeta = 0{\cdot}2$, $\gamma = 0{\cdot}3$)

Frequency component	Double HBM	FFT
DC component for x	8·256881	8·256882
DC component for y	−27·522936	−27·522940
ω_1	1·110939	1·110940
$2\omega_1$	$0{\cdot}2498 \times 10^{-5}$	$0{\cdot}4567 \times 10^{-5}$
$3\omega_1$	$1{\cdot}7347 \times 10^{-5}$	$1{\cdot}4986 \times 10^{-5}$

Meanwhile, in a non-linear rotor system with a cross-coupled stiffness, a self-excited vibration has been mentioned [11, 12]. The self-excited or internally resonant vibration is unpredictable since the internal resonant vibration frequency is neither the integer nor an integer multiple of the excitational forcing frequency. Due to internal resonant vibration, a rotor can rotate severely far below or far above the first critical speed. In particular, internal resonant rotor vibration is well represented as an *oil whirl* for a non-linear rotor system with hydraulic dynamic bearings [12]. Numerical integration is widely used to obtain the steady state solution and to study the stability criteria for these internally resonant vibrations. However, a more systematic procedure to obtain a steady state whirling response for the internal resonant rotor system has not been well addressed as yet.

In this paper, the direct HBM is generalized to multiple time scales, whereby the solution is expanded into a multiple Fourier series containing a number of frequencies that are incommensurable with one another. Theoretically, there is no limitation on the number of time scales used, and hence a very general aperiodic solution of any accuracy can be obtained if the proper frequencies and a sufficient number of corresponding harmonic terms are included. As the proposed method can directly detect the harmonic components involved, it is very straightforward to study the possible combination resonances or

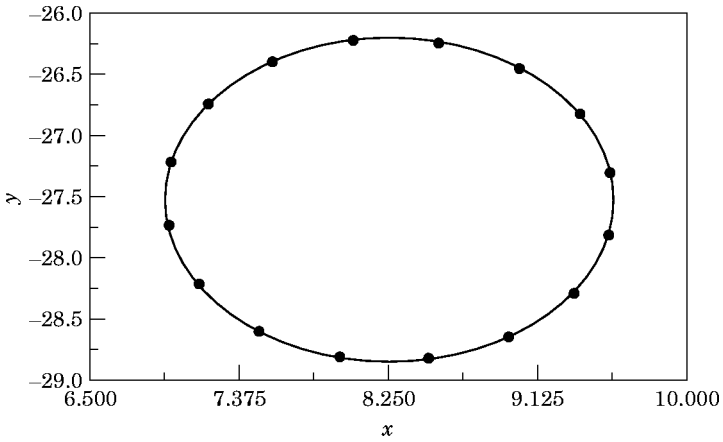

Figure 2. Synchronous whirling motion: $\Omega = 2$, $\alpha = 1{\cdot}0$, $\zeta = 0{\cdot}3$, $\gamma = 0{\cdot}3$. ——, Runge–Kutta; multiple HBM.

internal ones for the non-linear system. The aim of the present paper is primarily to introduce the essence of the new approach, and therefore only some important cases of a non-linear rotor problem are described to show the effectiveness of the method.

2. METHOD OF ANALYSIS

The equations of motion for a horizontal Jeffcott rotor with bearing clearances (see Figure 1) can be written as

$$mX'' + cX' + k_s X + Q_s Y + \Phi k_b X\left(1 - \frac{\delta}{\sqrt{X^2 + Y^2}}\right) - \mu \Phi k_b Y\left(1 - \frac{\delta}{\sqrt{X^2 + Y^2}}\right) = me\omega^2 \cos \omega t,$$

$$mY'' + cY' + k_s Y - Q_s X + \Phi k_b Y\left(1 - \frac{\delta}{\sqrt{X^2 + Y^2}}\right) + \mu \Phi k_b X\left(1 - \frac{\delta}{\sqrt{X^2 + Y^2}}\right) = me\omega^2 \sin \omega t - mg, \quad (1)$$

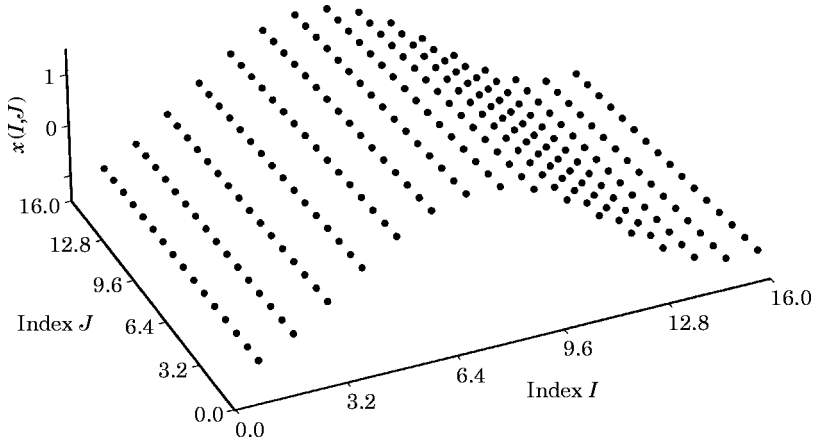

Figure 3. A three-dimensional view of displacement $x(\tau_1, \tau_2)$.

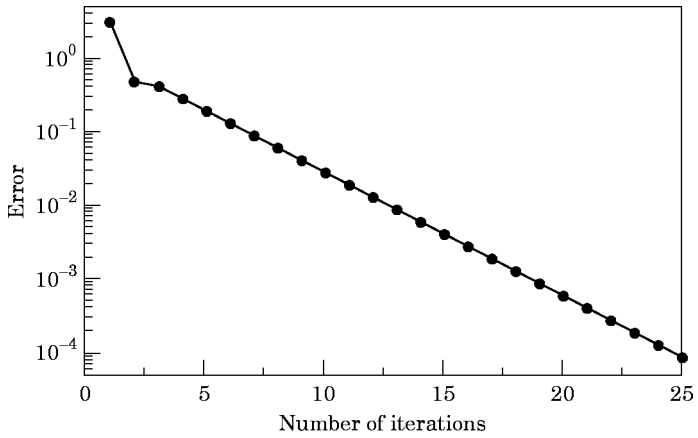

Figure 4. A convergence diagram: $\Omega = 2$, $\alpha = 1{\cdot}0$, $\zeta = 0{\cdot}2$, $\gamma = 0{\cdot}4$.

where k_s is the shaft stiffness, Q_s is the cross-coupling stiffness, c is the system damping, μ is the friction coefficient, and δ is the radial clearance of the bearing. A prime denotes a derivative with respect to time t and the discrete function Φ has the form

$$\Phi = \begin{cases} 1, & \sqrt{X^2 + Y^2} > \delta, \\ 0, & \sqrt{X^2 + Y^2} \leqslant \delta. \end{cases}$$

To study the effect of the parameters on the behavior of the system, the following non-dimensional groups are introduced: $\omega_n = \sqrt{K/m}$, $K = 4k_sk_b/(\sqrt{k_2} + \sqrt{k_b})^2$, $x = X/\epsilon$, $y = Y/\epsilon$, $\Omega = \omega/\omega_n$, $\zeta = c/2m\omega_n$, $\gamma = Q_s/K$, $\alpha = k_b/k_s$, $\delta^* = \delta/\epsilon$, $\phi = g/\omega_n^2\epsilon$, $r^* = \sqrt{x^2 + y^2}$ and $v\theta = \omega t$. Here v denotes the subharmonic ratio ($v = 1$ for the harmonic case, and $v = n$ for an nth subharmonic case). Equation (4) can be written as

$$\ddot{x} + 2\zeta \frac{v}{\Omega}\dot{x} + \frac{(v^2/\Omega^2)(1 + \sqrt{\alpha})^2}{4\alpha} x + \gamma \frac{v^2}{\Omega^2} y + T(\theta) - \mu F(\theta) = v^2 \cos v\theta,$$

$$\ddot{y} + 2\zeta \frac{v}{\Omega}\dot{y} + \frac{(v^2/\Omega^2)(1 + \sqrt{\alpha})^2}{4\alpha} + T(\theta)y - \gamma \frac{v^2}{\Omega^2} x + \mu T(\theta) = v^2 \sin v\theta - \phi \frac{v^2}{\Omega^2}, \quad (2)$$

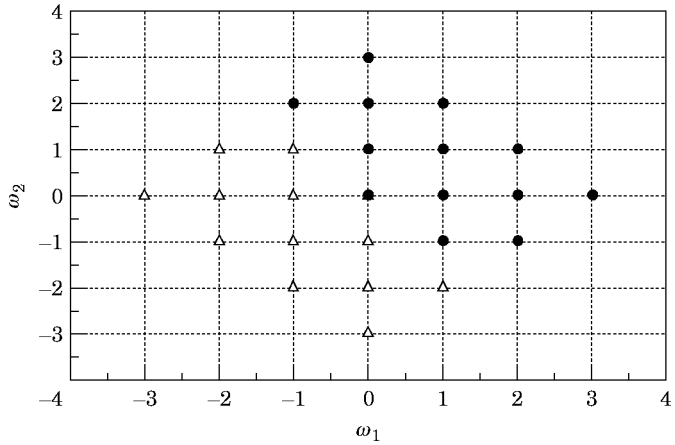

Figure 5. A geometrical interpretation of the frequency components satisfying equations (24) and (25).

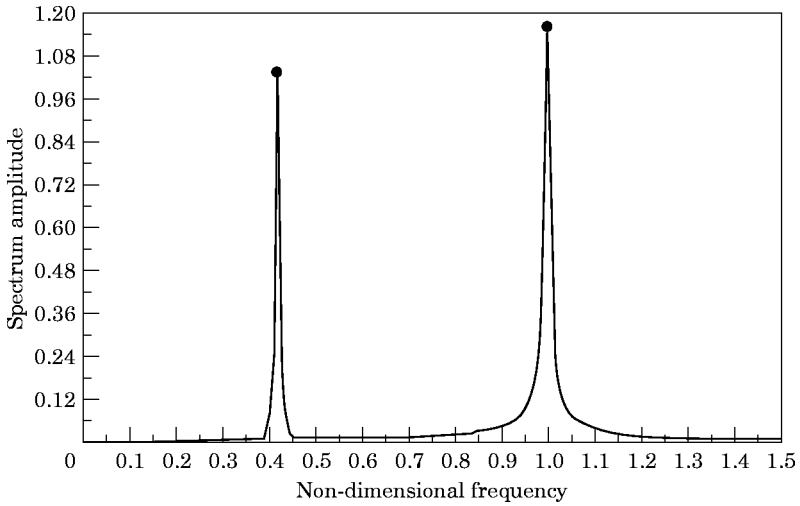

Figure 6. The power spectrum of the internal resonance motion: $\Omega = 2$, $\alpha = 1{\cdot}0$, $\zeta = 0{\cdot}2$, $\gamma = 0{\cdot}4$. ——, Numerical integration; •, multiple HBM.

where a dot represents a derivative with respect to dimensionless time θ and Φ are unity if r^* is greater than δ^*; otherwise, they are zero. $T(\theta)$ and $F(\theta)$ are given by the following expressions:

$$T(\theta) = \Phi \frac{v^2}{\Omega^2} \frac{(1+\sqrt{\alpha})^2}{4} x\left(1 - \frac{\delta^*}{\sqrt{x^2+y^2}}\right),$$

$$F(\theta) = \Phi \frac{v^2}{\Omega^2} \frac{(1+\sqrt{\alpha})^2}{4} y\left(1 - \frac{\delta^*}{\sqrt{x^2+y^2}}\right), \tag{3}$$

where

$$\Phi = \begin{cases} 1, & \sqrt{x^2+y^2} > \delta^*, \\ 0, & \sqrt{x^2+y^2} \leqslant \delta^*. \end{cases}$$

In periodic vibration, all frequencies are commensurable and, therefore, it is reasonable to postulate that internal resonant motion could be made up of components with incommensurable frequencies. Therefore, the solution of equations (1) and (2) can be regarded as functions of $\omega_1\theta$ and $\omega_2\theta$; i.e.,

$$x = x(\omega_1\theta, \omega_2\theta), \tag{4}$$

where the frequencies ω_1 and ω_2 are incommensurable with one another in general. It is reported that the incommensurable frequency component occurs as a result of the cross-coupling stiffness terms in equation (2), and the second incommensurable frequency component, ω_2, can be easily obtained as

$$\omega_2^2 = \frac{(\beta - \zeta^2)}{2\Omega^2} \pm \frac{1}{2\Omega^2}[(\zeta^2 - \beta)^2 + \gamma^2]^{1/2}, \tag{5}$$

where $\beta = (1+\sqrt{\alpha})^2/4\alpha$. It should be noted that $\omega_1 = 1$ and that the positive sign of ω_2 is used in the paper.

By introducting

$$\tau_k = \omega_k \theta, \qquad k = 1, 2, \tag{6}$$

within the new time domain, where $0 \leqslant \tau_k \leqslant 2\pi$ ($k = 1, 2$), equation (5) can be rewritten as

$$x = x(\tau_1, \tau_2). \tag{7}$$

Since τ_j ($j = 1, 2$) are functions of t, the following operator relations can be obtained:

$$\frac{\mathrm{d}}{\mathrm{d}\theta} = \omega_1 \frac{\mathrm{d}}{\mathrm{d}\tau_1} + \omega_2 \frac{\mathrm{d}}{\mathrm{d}\tau_2},$$

$$\frac{\mathrm{d}^2}{\mathrm{d}\theta^2} = \omega_1^2 \frac{\mathrm{d}^2}{\mathrm{d}\tau_1^2} + \omega_2^2 \frac{\mathrm{d}^2}{\mathrm{d}\tau_2^2} + 2\omega_1\omega_2 \frac{\mathrm{d}^2}{\mathrm{d}\tau_1\,\mathrm{d}\tau_2}. \tag{8}$$

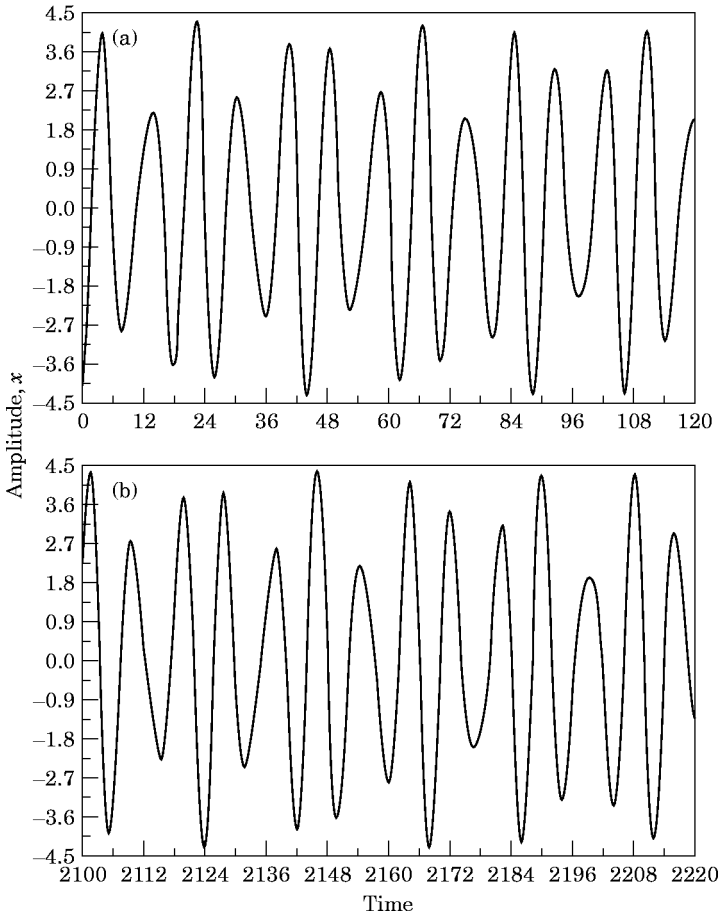

Figure 7. (a) The time response of the x displacement using multiple HBM. (b) The time response of the x displacement using numerical integration. $\Omega = 2$, $\alpha = 1{\cdot}0$, $\zeta = 0{\cdot}2$, $\gamma = 0{\cdot}4$.

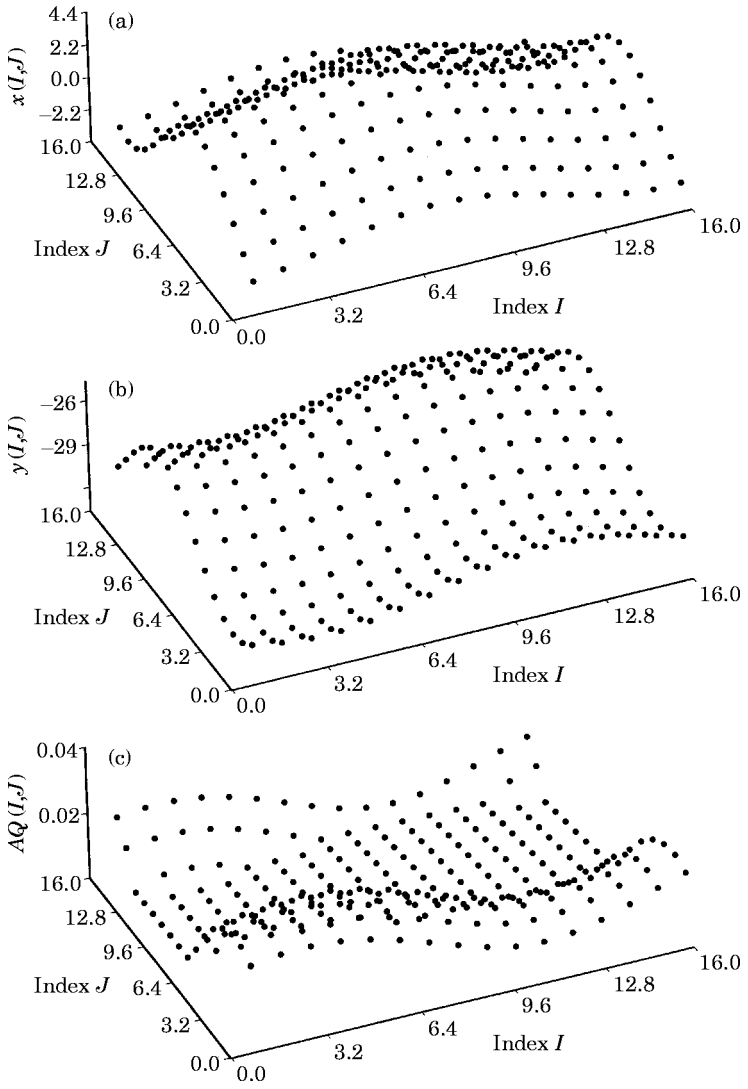

Figure 8. Three-dimensional views of (a) the displacement $x(\tau_1, \tau_2)$, (b) the displacement $y(\tau_1, \tau_2)$ and (c) the restoring force component $A(\tau_1, \tau_2)$.

Substituting equation (7) into equation (2) leads to

$$\omega_1^2 \frac{d^2x}{d\tau_1^2} + 2\omega_1\omega_2 \frac{d^2x}{d\tau_1\, d\tau_2} + \omega_2^2 \frac{d^2x}{d\tau_2^2} + \frac{2\zeta v}{\Omega}\left(\omega_1 \frac{dx}{d\tau_1} + \omega_2 \frac{dx}{d\tau_2}\right)\frac{v^2}{\Omega^2}\frac{(1+\sqrt{\alpha})^2}{4\alpha}\, x$$

$$+ \gamma \frac{v^2}{\Omega^2} y + T(x, y) - \mu F = v^2 \cos \tau_1,$$

$$\omega_1^2 \frac{d^2y}{d\tau_1^2} + 2\omega_1\omega_2 \frac{d^2y}{d\tau_1\, d\tau_2} + \omega_2^2 \frac{d^2y}{d\tau_2^2} + \frac{2\zeta v}{\Omega}\left(\omega_1 \frac{dy}{d\tau_1} + \omega_2 \frac{dy}{d\tau_2}\right)\frac{v^2}{\Omega^2}\frac{(1+\sqrt{\alpha})^2}{4\alpha}\, y - \gamma \frac{v^2}{\Omega^2} x$$

$$+ F(x, y) + \mu F(x, y) = v^2 \sin \tau_1 - \phi \frac{v^2}{\Omega^2}. \tag{9}$$

Using the two-dimensional frequency concept, the two-dimensional discrete time solution for x and y in equation (9) with the (m, n)th component can be expanded as follows:

$$x(m,n) = \sum_{k=-M}^{M} \sum_{l=-M}^{M} \left\{ a_{xkl} \cos \frac{2\pi}{N} (mk + nl) - b_{xkl} \sin \frac{2\pi}{N} (mk + nl) \right\}$$

$$= \sum_{k=-M}^{M} \sum_{l=-M}^{M} \left\{ a_{xkl} \cos (k\tau_1 + l\tau_2) - b_{xkl} \cos (k\tau_1 + l\tau_2) \right\}, \tag{10a}$$

$$y(m,n) = \sum_{k=-M}^{M} \sum_{l=-M}^{M} \left\{ a_{ykl} \cos \frac{2\pi}{N} (mk + nl) - b_{ykl} \sin \frac{2\pi}{N} (mk + nl) \right\}$$

$$= \sum_{k=-M}^{M} \sum_{l=-M}^{M} \left\{ a_{ykl} \cos (k\tau_1 + l\tau_2) - b_{ykl} \cos (k\tau_1 + l\tau_2) \right\}, \tag{10b}$$

where M represents the number of retained harmonic terms and N is the number of discrete time steps. Remember that the indices m and n vary from 1 to N, respectively, in the discrete time domain, and that k and l vary from $-M$ to M, respectively, in the discrete frequency domain. Equation (10) is the expression of the two-dimensional time domain of the IDFT (inverse discrete Fourier transform). Similarly, the non-linear restoring forces of $T(\theta)$ and $F(\theta)$ in equation (2) with the (m, n)th discrete time domain can be expanded assuming that $T(\theta)$ and $F(\theta)$ have the same double harmonic components as

$$T(x,y)(m,n) = \sum_{k=-M}^{M} \sum_{l=-M}^{M} \left\{ c_{xkl} \cos \frac{2\pi}{N} (mk + nl) - d_{xkl} \sin \frac{2\pi}{N} (mk + nl) \right\}, \tag{11a}$$

$$F(x,y)(m,n) = \sum_{k=-M}^{M} \sum_{l=-M}^{M} \left\{ c_{ykl} \cos \frac{2\pi}{N} (mk + nl) - d_{ykl} \sin \frac{2\pi}{N} (mk + nl) \right\}. \tag{11b}$$

It should be noted that the concepts of the two-dimensional frequency and the two-dimensional discrete time domain are clearly an extended version of the DFT (discrete Fourier transform) and the IDFT of a single input non-linear system. Also, the non-linear forcing terms, $T(x, y)(m, n)$ and $F(x, y)(m, n)$, in equation (11) are functions of the discrete displacements, $x(m, n)$ and $y(m, n)$, in equation (10), satisfying equation (3) in the (m, n)th time domain. Therefore, the unknown coefficients of c_{xkl}, c_{ykl}, d_{xkl} and d_{ykl} in

equation (11) can be expressed using the unknown coefficients of a_{xkl}, a_{xkl} and b_{ykl} in the two-dimensional discrete time domain, as

$$T(k,l)(m,n) = \begin{cases} \dfrac{v^2}{\Omega^2}\dfrac{(1+\sqrt{\alpha})^2}{4}\,x(m,n)\left(1-\dfrac{\delta^*}{\sqrt{x(m,n)^2+y(m,n)^2}}\right), & \sqrt{x(m,n)^2+y(m,n)^2} > \delta^*, \\ 0, & \sqrt{x(m,n)^2+y(m,n)^2} \leqslant \delta^*, \end{cases}$$

$$F(k,l)(m,n) = \begin{cases} \dfrac{v^2}{\Omega^2}\dfrac{(1+\sqrt{\alpha})^2}{4}\,y(m,n)\left(1-\dfrac{\delta^*}{\sqrt{x(m,n)^2+y(m,n)^2}}\right), & \sqrt{x(m,n)^2+y(m,n)^2} > \delta^*, \\ 0, & \sqrt{x(m,n)^2+y(m,n)^2} \leqslant \delta^*, \end{cases} \tag{12}$$

The unknown coefficients $c(k,l)$ and $d(k,l)$ can easily be obtained as

$$c_{xkl} = \frac{2}{N^2}\sum_{n=0}^{N}\sum_{n=0}^{N} T(x,y)(m,n)\cos\frac{2\pi}{N}(mk+nl),$$

$$c_{ykl} = \frac{2}{N^2}\sum_{n=0}^{N}\sum_{n=0}^{N} T(x,y)(m,n)\sin\frac{2\pi}{N}(mk+nl),$$

$$d_{xkl} = \frac{2}{N^2}\sum_{n=0}^{N}\sum_{n=0}^{N} F(x,y)(m,n)\cos\frac{2\pi}{N}(mk+nl),$$

$$d_{ykl} = \frac{2}{N^2}\sum_{n=0}^{N}\sum_{n=0}^{N} F(x,y)(m,n)\sin\frac{2\pi}{N}(mk+nl), \tag{13}$$

where k and l vary from $-M$ to M. If more than two input exciting frequencies are involved in the system, it is only necessary to include more adequate harmonic or time elements in equations (10–13). Substituting equations (10) and (11) into equation (2) and rearranging the terms with the same trigonometric elements leads to the following:

(i) for constant terms,

$$\frac{v^2}{\Omega^2}\frac{(1+\sqrt{a})^2}{4\alpha}\,a_{x0} + \gamma\frac{v^2}{\Omega^2}\,a_{y0} + C_{x0} - \mu c_{y0} = 0,$$

$$\frac{v^2}{\Omega^2}\frac{(1+\sqrt{\alpha})^2}{4\alpha}\,a_{y0} - \gamma\frac{v^2}{\Omega^2}\,a_{x0} + c_{y0} + \mu c_{x0} + \phi\frac{v^2}{\Omega^2} = 0; \tag{14}$$

(ii) for trigonometric terms

$$-\left(k^2\omega_1^2 + 2kl\omega_1\omega_2 + l^2\omega_2^2 + \frac{v^2}{\Omega^2}\frac{(1+\sqrt{\alpha})^2}{4\alpha}\right)a_{xkl} - \left(\frac{2\zeta v}{\Omega}\omega_1 k + \frac{2\zeta v}{\Omega}\omega_2 l\right)b_{xkl}$$

$$+ \gamma\frac{v^2}{\Omega^2}a_{ykl} + c_{xkl} - \mu c_{ykl} - v^2\Phi_1(\cos\tau_1) = 0,$$

$$\left(k^2\omega_1^2 + 2kl\omega_1\omega_2 + l^2\omega_2^2 - \frac{v^2}{\Omega^2}\frac{(1+\sqrt{\alpha})^2}{4\alpha}\right)b_{xkl} - \left(\frac{2\zeta v}{\Omega}\omega_1 k + \frac{2\zeta v}{\Omega}\omega_2 l\right)a_{xkl}$$

$$-\gamma\frac{v^2}{\Omega^2}b_{ykl} - d_{xkl} + \mu d_{ykl} = 0,$$

$$-\left(k^2\omega_1^2 + 2kl\omega_1\omega_2 + l^2\omega_2^2 - \frac{v^2}{\Omega^2}\frac{(1+\sqrt{\alpha})^2}{4\alpha}\right)a_{ykl} - \left(\frac{2\zeta v}{\Omega}\omega_1 k + \frac{2\zeta v}{\Omega}\omega_2 l\right)b_{ykl}$$

$$-\gamma\frac{v^2}{\Omega^2}a_{xkl} + c_{ykl} + \mu c_{xkl} = 0,$$

$$-\left(k^2\omega_1^2 + 2kl\omega_1\omega_2 + l^2\omega_2^2 + \frac{v^2}{\Omega^2}\frac{(1+\sqrt{\alpha})^2}{4\alpha}\right)a_{xkl} - \left(\frac{2\zeta v}{\Omega}\omega_1 k + \frac{2\zeta v}{\Omega}\omega_2 l\right)b_{xkl}$$

$$+ \gamma\frac{v^2}{\Omega^2}a_{ykl} + c_{xkl} - \mu c_{ykl} - v^2\Phi_1(\cos\tau_1) = 0, \tag{15}$$

where $(k, l = -M, -M+1, \ldots, M-1, M)$, and Φ_1 is 1 if $v = k$ and $l = 0$ and otherwise is zero. By combining all the equations of (14) and (15), the following non-linear algebraic equations can be obtained:

$$g_1 = \frac{v^2}{\Omega^2}\frac{(1+\sqrt{\alpha})^2}{4\alpha}a_{x0} + \gamma\frac{v^2}{\Omega^2}a_{y0} + c_{x0} - \mu c_{y0} = 0,$$

$$\vdots$$

$$g_{16k+4l-1} = -\left(k^2\omega_1^2 + 2kl\omega_1\omega_2 + l^2\omega_2^2 + \frac{v^2}{\Omega^2}\frac{(1+\sqrt{\alpha})^2}{4\alpha}\right)a_{xkl} - \left(\frac{2\zeta v}{\Omega}\omega_1 k + \frac{2\zeta v}{\Omega}\omega_2 l\right)b_{xkl}$$

$$+ \gamma\frac{v^2}{\Omega^2}a_{ykl} + c_{xkl} - \mu c_{ykl} - v^2\Phi_1(\cos\tau_1) = 0,$$

$$g_{16k+4l} = \left(k^2\omega_1^2 + 2kl\omega_1\omega_2 + l^2\omega_2^2 - \frac{v^2}{\Omega^2}\frac{(1+\sqrt{\alpha})^2}{4\alpha}\right)b_{xkl} - \left(\frac{2\zeta v}{\Omega}\omega_1 k + \frac{2\zeta v}{\Omega}\omega_2 l\right)a_{xkl}$$

$$-\gamma\frac{v^2}{\Omega^2}b_{ykl} - d_{xkl} + \mu d_{ykl} = 0, \tag{16}$$

$$\vdots$$

where $k, l = -M, -M+1, \ldots, M-1, M$.

Equation (16) is implicitly non-linear: therefore, a numerical iteration scheme such as the Newton–Raphson method can be applied to obtain the solution. In equation (16) the only unknowns are $a_{xkl}, a_{ykl}, b_{xkl}, \ldots, b_{ykl}$ and the coefficients of $c_{xkl}, c_{ykl}, d_{xkl}, \ldots, d_{ykl}$ are easily obtained using equations (12) and (13). In obtaining the non-linear algebraic equations using HBM, Ushida and Chua [4] used one-dimensional frequency and the time domain concept to obtain multi-input frequency systems, resulting in more unknown coefficients than the number of algebraic equations during the process of transformation between DFT and IDFT. As they utilized the least squares method to guess the extra unknowns for the unknown harmonic coefficients, this inherently involves ill-conditioning problems unless very elaborate and lengthy discrete time steps are selected. However, the two-dimensional frequency domain approach proposed in this paper presents no difficulties in the transformation process between the DFT and the IDFT using the Galerkin technique, nor problems in representing non-linear force terms with assumed harmonic components. It can always offer a very accurate Jacobian matrix which gives the convergent solution for the iteration scheme.

If the vectors $\{p\}$ and $\{q\}$ represent the unknown components in equation (16), as

$$\{p\} = [a_{x00}, a_{y00}, a_{x01}, b_{x01}, a_{y01}, b_{y01}, \ldots, a_{yij}, b_{yij}]^{\mathrm{T}}, \tag{17a}$$

$$\{q\} = [c_{x00}, c_{y00}, c_{x01}, d_{x01}, c_{y01}, d_{y01}, \ldots, c_{yii}, d_{yij}]^{\mathrm{T}}, \tag{17b}$$

then the vector $\{q\}$ can be represented from the unknown vector $\{p\}$ using the Galerkin technique, which implies a double integral from 0 to 2π in arguments τ_1 and τ_2, respectively, as

$$\begin{aligned}
&\int_0^{T_2}\int_0^{T_1} \{c_{xkl}\cos(k\tau_1 + l\tau_2) - d_{xkl}\sin(k\tau_1 + l\tau_2)\} \\
&\qquad \times [\ldots, \cos(k\tau_1 + l\tau_2), \ldots, \sin(k\tau_1 + l\tau_2), \ldots]^{\mathrm{T}}\,\mathrm{d}\tau_1\,\mathrm{d}\tau_2 \\
&\quad = \int_0^{T_2}\int_0^{T_1} A\{a_{xmn}\cos(m\tau_1 + n\tau_2) - b_{xmn}\sin(m\tau_1 + n\tau_2)\} \\
&\qquad \times [\ldots, \cos(k\tau_1 + l\tau_2), \ldots, \sin(k\tau_1 + l\tau_2), \ldots]^{\mathrm{T}}\,\mathrm{d}\tau_1\,\mathrm{d}\tau_2 \\
&\qquad - \int_0^{T_2}\int_0^{T_1} B\{a_{ymn}\cos(m\tau_1 + n\tau_2) - b_{ymn}\sin(m\tau_1 + n\tau_2)\} \\
&\qquad \times [\ldots, \cos(k\tau_1 + l\tau_2), \ldots, \sin(k\tau_1 + l\tau_2), \ldots]^{\mathrm{T}}\,\mathrm{d}\tau_1\,\mathrm{d}\tau_2, \\
&\int_0^{T_2}\int_0^{T_1} \{c_{ykl}\cos(k\tau_1 + l\tau_2) - d_{ykl}\sin(k\tau_1 + l\tau_2)\} \\
&\qquad \times [\ldots, \cos(k\tau_1 + l\tau_2), \ldots, \sin(k\tau_1 + l\tau_2), \ldots]^{\mathrm{T}}\,\mathrm{d}\tau_1\,\mathrm{d}\tau_2 \\
&\quad = \int_0^{T_2}\int_0^{T_1} -C\{a_{xmn}\cos(m\tau_1 + n\tau_2) - b_{xmn}\sin(m\tau_1 + n\tau_2)\} \\
&\qquad \times [\ldots, \cos(k\tau_1 + l\tau_2), \ldots, \sin(k\tau_1 + l\tau_2), \ldots]^{\mathrm{T}}\,\mathrm{d}\tau_1\,\mathrm{d}\tau_2 \\
&+ \int_0^{T_2}\int_0^{T_1} D\{a_{ymn}\cos(m\tau_1 + n\tau_2) - b_{ymn}\sin(m\tau_1 + n\tau_2)\} \\
&\qquad \times [\ldots, \cos(k\tau_1 + l\tau_2), \ldots, \sin(k\tau_1 + l\tau_2), \ldots]^{\mathrm{T}}\,\mathrm{d}\tau_1\,\mathrm{d}\tau_2,
\end{aligned} \tag{18}$$

where

$$A = \Phi \frac{v^2}{\Omega^2}\left[\frac{(1+\sqrt{\alpha})^2}{4}\frac{(1+\sqrt{\alpha})^2}{4}\,\delta^*(x^2+y^2)^{-3/2}y^2\right],$$

$$C = D = \Phi \frac{v^2}{\Omega^2}\left[\frac{(1+\sqrt{\alpha})^2}{4}\frac{(1+\sqrt{\alpha})^2}{4}\,\delta^*(x^2+y^2)^{-3/2}xy\right],$$

$$D = \Phi \frac{v^2}{\Omega^2}\left[\frac{(1+\sqrt{\alpha})^2}{4}\frac{(1+\sqrt{\alpha})^2}{4}\,\delta^*(x^2+y^2)^{-3/2}x^2\right].$$

The above relations can lead to solutions that can be summarized in discrete form as

$$\frac{\partial c_{xkl}}{\partial a_{xmn}} = \frac{2}{N^2}\sum_{i=0}^{N}\sum_{j=0}^{N} A_{ij}\cos\frac{2\pi(ik+jl)}{N}\cos\frac{2\pi(im+jn)}{N},$$

$$\frac{\partial d_{xkl}}{\partial b_{ymn}} = -\frac{2}{N^2}\sum_{i=0}^{N}\sum_{j=0}^{N} -B_{ij}\sin\frac{2\pi(ik+jl)}{N}\sin\frac{2\pi(im+jn)}{N},$$

$$\frac{\partial c_{ykl}}{\partial a_{xmn}} = -\frac{2}{N^2}\sum_{i=0}^{N}\sum_{j=0}^{N} C_{ij}\cos\frac{2\pi(ik+jl)}{N}\cos\frac{2\pi(im+jn)}{N},$$

$$\frac{\partial d_{ykl}}{\partial b_{ymn}} = \frac{2}{N^2}\sum_{i=0}^{N}\sum_{j=0}^{N} D_{ij}\sin\frac{2\pi(ik+jl)}{N}\sin\frac{2\pi(im+jn)}{N}, \tag{19}$$

where A_{ij}, B_{ij}, C_{ij} and D_{ij} are discrete time versions of A, B, C and D of equation (18). In the above equations, the coefficients A, B, C and D represent the non-dimensional discontinuous stiffness depending on Φ, where $\Phi = 1$ when the rotor contacts with its housing and is otherwise zero when no contact occurs.

The non-linear algebraic equations can be solved using the iteration technique. One of the most frequently used iteration processes is the Newton–Raphson method, if an explicit Jacobian matrix is obtained from the given non-linear equations. Fortunately, our problem considered in this paper is capable of obtaining the exact Jacobian terms using the Galerkin procedure, as addressed before. The iteration procedure can be described by

$$\{p\}^i = \{p\}^{i-1} - [J]^{-1}\{G\}^{i-1}, \tag{20}$$

where the superscript i denotes the ith iteration step during the iteration process, $\{G\}$ is a column vector having the elements of equation (16), and $[J]$ is the Jacobian matrix, which has the components

$$[J] = [J_1] + [J_2], \tag{21}$$

where

$$[J_1] = \begin{bmatrix} \cdots & t_1 - i^2\omega_1^2 & -t_2(i\omega_1 + j\omega_2) & t_3 & 0 & \\ & -2ij\omega_1\omega_2 - j^2\omega_2^2 & & & & \\ \cdots & -t_2(i\omega_1 + j\omega_2) & -t_1 + i^2\omega_1^2 & 0 & -t_3 & \cdots \\ & & +2ij\omega_1\omega_2 + j^2\omega_2^2 & & & \\ \cdots & -t_3 & 0 & t_1 - i^2\omega_1^2 & -t_2(i\omega_1 + j\omega_2) & \cdots \\ & & & -2ij\omega_1\omega_2 - j^2\omega_2^2 & & \\ \cdots & 0 & t_3 & -t_2(i\omega_1 + j\omega_2) - 2ij\omega_1\omega_2 - j^2\omega_2^2 & t_1 - i^2\omega_1^2 & \cdots \end{bmatrix} \tag{22}$$

and

$$[J_2] = \begin{bmatrix} \dfrac{\partial c_{x0}}{\partial a_{x0}} & \dfrac{\partial c_{x0}}{\partial a_{y0}} & \dfrac{\partial c_{x0}}{\partial a_{x01}} & \dfrac{\partial c_{x0}}{\partial b_{x01}} & \cdots & \dfrac{\partial c_{x0}}{\partial b_{ymm}} \\ \dfrac{\partial c_{y0}}{\partial a_{x0}} & \dfrac{\partial c_{y0}}{\partial a_{y0}} & \dfrac{\partial c_{y0}}{\partial a_{x01}} & \dfrac{\partial c_{y0}}{\partial b_{x01}} & \cdots & \dfrac{\partial c_{y0}}{\partial b_{ymm}} \\ \vdots & \vdots & \vdots & \vdots & \ddots & \vdots \\ \dfrac{\partial d_{ymn}}{\partial a_{x0}} & \dfrac{\partial d_{ymn}}{\partial a_{y0}} & \dfrac{\partial d_{ymn}}{\partial a_{x01}} & \dfrac{\partial d_{ymn}}{\partial a_{y01}} & \cdots & \dfrac{\partial d_{ymn}}{\partial b_{ymm}} \end{bmatrix}, \tag{23}$$

in which

$$t_1 = \frac{v^2}{\Omega^2}\frac{(1+\sqrt{\alpha})^2}{4\alpha}, \qquad t_2 = \frac{2\zeta v}{\Omega} \quad \text{and} \quad t_3 = \gamma\frac{v^2}{\Omega^2}.$$

From equations (22) and (23), it is clear that the Jacobian matrix is explicitly expressed with trigonometric functions. By rendering it explicit, the iteration process can always offer convergent solutions if the parameters considered are located within the well-conditioned ranges.

3. NUMERICAL RESULTS

For illustration, the methods developed in this study are applied to a non-linear Jeffcott rotor with piecewise-linear bending characteristics. Due to the stiffness cross-coupling terms in equation (1), it is widely known that the linear or non-linear rotor system with cross-coupling force terms might lead to an unstable synchronous or unsynchronous whirl. A prior systematic bifurcation study showed that a Hopf bifurcation leading to internal resonant vibration with a single excitational input did occur, depending on the cross-coupling stiffness coefficients [13]. In reference [13], the unstable unsynchronous whirl appeared through Hopf bifurcation in which an internal resonance was developed independent of the excitational whirl frequency. Usually, the second frequency induced by internal resonance is not an integer fraction of an excitational whirl frequency (due to the unbalance force), and hence it is very difficult to analyze further using the method developed by Kim and Noah. Some researchers have tried to locate and separate internal resonant frequencies through various numerical methods or experimental work for a non-linear rotor system. Their methods have been partly successful in isolating internal resonant non-linear frequencies; however, the conventional FFT algorithm was used after numerical integration in identifying the internal resonance [14]. The rotor system considered here is a truly two-dimensional system in which cross-coupling terms and

non-linear restoring forces due to gap changes are expressed through two-directional displacements, and the proposed method directly offers frequency components for internal resonances.

The accuracy of the proposed method is first verified by comparison with the results of the frequency components from FFT, in which 8192 discrete time data points from numerical integration were used. In Tables 1–3 is shown the comparison between the results of the two methods, in which no internal resonance occurs since the non-dimensional cross-coupling stiffness coefficient term, γ, is not large enough to induce an internal resonant fractional frequency. The tables show that the proposed method gives very accurate frequency components when no internal resonance occurs.

A polar plot for the case of Table 1 ($\Omega = 2$, $\alpha = 1{\cdot}0$, $\zeta = 0{\cdot}3$ and $\gamma = 0{\cdot}3$) was displayed as shown in Figure 2. In the figure, dots represent the responses obtained by double HBM and the solid line denotes the results of numerical integration. As the present HBM separates the real time domain into two *hyper-time* domains, in which each period varies from 0 to 2π, respectively, the amplitudes of $x(\tau_1, \tau_2)$ can be viewed three-dimensionally in each hyper-time domain as shown in Figure 3. In the figure, the same non-dimensional parameters were used as in Figure 2. Each mutual perpendicular horizontal axis represents the hyper-time domain of τ_1 and τ_2 having a period of 2π. The figure also shows that the amplitude of the i axis, which represents the first argument of τ_1, varies as the hyper-time changes. However, the second argument of τ_2 does not contribute to the amplitude change. This is true since the non-dimensional parameters utilized in this example show only periodic synchronous whirling responses; i.e., only the involvement of whirling with the τ_1 argument. In most simulation cases with parameter ranges used in Tables 1–3, the maximum four iteration steps were enough to obtain synchronous whirling responses within considerable accuracy with an error bound of 1×10^{-6}. However, if the internal resonant frequency is involved in the whirling response as the cross-coupling term γ exceeds certain values, the iteration process slows down to obtain the solution within the required error bound. The convergence rates for this case are shown in Figure 4. In the figure, non-dimensional parameters of $\Omega = 2{\cdot}0$, $\alpha = 1{\cdot}0$, $\zeta = 0{\cdot}2$ and $\gamma = 0{\cdot}4$ were used. In most simulation cases more than 15 iterations were needed to obtain internal resonant non-synchronous whirling within a certain error bound.

To find an adequate number of harmonic components of each input frequency in this example, various numerical experiments were carried out. The combination of each frequency component might be expressed as

$$\pm k\tau_1 \pm l\tau_2, \tag{24}$$

where k and l include all integers and satisfy

$$|k| + |l| < B \qquad \text{and} \qquad \pm k\tau_1 \pm l\tau_2 > 0 \tag{25}$$

for a properly chosen integer value B. The frequency component satisfying equations (24) and (25) can be represented geometrically by dots in the frequency diagram, as shown in Figure 5. Here, each solid dot located at (k, l) corresponds to a frequency component $\pm k\tau_1 \pm l\tau_2$ satisfying equation (25), and the other empty upper triangle marks are frequency components excluded in equation (24). The decision on how many harmonic components to include for each frequency term in this example has been made from the numerical experiments. From various numerical experiments, the integer value of B and the non-dimensional discrete time number N are taken as 3 and 16, respectively, and good results were obtained, as shown in Figure 2 and Tables 1–3. If one takes the larger value of B, the corresponding accuracy of the method will be better. However, the computational speed will be much slower and more memory space will be needed.

One of the main advantages of this proposed method is the direct decomposition of each frequency component, which makes it easy to study the coupling effects (i.e., internal resonance or combination resonance) for the given non-linear Jeffcott rotor system. A comparison between the doubly harmonic balance method and numerical integration in the frequency domain is shown in Figure 6, with the same parameters as used in Figure 4. The figure shows good agreement between the two methods in the frequency domain. Only the excitational frequency ω_1 is involved for the unbalance response; the non-integer fractional frequency ω_2 appears suddenly ($\omega_2 = 0{\cdot}42$), which implies that the non-linear rotor system gets into severe non-synchronous whirling even though the rotor does not pass the first critical speed due to the cross-coupling force terms.

The time history for x-directional response with a non-integer fractional frequency is calculated in the discrete time domain from the frequency response of the multiple HBM, as shown in Figure 7(a). The time response is compared with that from numerical integration, as displayed in Figure 7(b). Both figures reveal that the doubly harmonic balance method can offer very accurate results for the non-linear system considered here in the time and frequency domains. In Figure 7(b) sufficient time should be allowed to obtain steady state whirling due to low damping. However, doubly HBM directly offers a steady state response without regard to the damping terms. In Figure 8(a) is shown the three-dimensional x-axis response for the non-integer fractional frequency case. The figure clearly shows that each argument of τ_1 and τ_2 varies from 0 to 2π, separately. As non-linear contacts happen in all directions (i.e., both the x and y directions), the y-axis response also shows double periodic changes, as shown in Figure 8(b). The non-linear restoring force term $A(\tau_1, \tau_2)$ is displayed in each hyper-time domain, as shown in Figure 8(c). As the non-linear forcing term of $A(\tau_1, \tau_2)$ has a discontinuous characteristic depending on the contact conditions, as expressed in equation (12), the figure clearly shows the discontinuous function for the restoring force element.

4. CONCLUSIONS

The doubly harmonic balance method is developed and applied to the two-dimensional non-linear Jeffcott rotor system to show its effectiveness and accuracy. The method is proved to be superior in obtaining direct frequency components as compared with numerical integration for a high damping system. Although a detailed internal resonance analysis was not performed in this paper, the present method can serve as a tool to examine internal or combinational resonant vibration for a non-linear rotor with parameter variations. Moreover, the proposed method can be extended to apply easily to a two-dimensional system with multiple exciting input frequencies, such as a dual- or triple-rotor system.

ACKNOWLEDGMENT

This work was carried out as part of the research projects supported by KOSEF (Korean Science & Engineering Foundation; No. 1-1002-001-2). The authors are grateful for this support.

REFERENCES

1. A. H. Nayfeh and D. T. Mook 1979 *Nonlinear Oscillations*. New York: Wiley-Interscience.
2. Y. B. Kim and S. T. Noah 1991 *Transactions of the American Society of Mechanical Engineers, Journal of Applied Mechanics* **58**, 543–553. Stability and bifurcation analysis of oscillators with piecewise-linear characteristics: a general approach.

3. S. L. Lau, Y. K. Cheung and S. Y. Wu 1983 *ASME Paper* 83-*WA*/*APM*-7. Incremental harmonic balance method with multiple time scales for aperiodic vibrations of nonlinear systems.
4. Ushida and L. O. Chua 1984 *IEEE Transactions on Circuits and Systems* **CAS-31**, 766–778. Frequency-domain analysis of nonlinear circuits driven by multi-tone signals.
5. Kaas-Petersen 1985 *Physics* **58**, 395–403. Computation of quasi-periodic solutions of forced dissipative systems.
6. Kaas-Petersen 1987 *Physics* **25D**, 286–306. Computation, continuation, and bifurcation of true solutions for dissipative maps and ordinary differential equations.
7. F. H. Ling 1991 *Journal of Sound and Vibration* **144**, 293–304. Quasi-periodic solutions calculated with simple shooting technique.
8. Y. B. Kim 1996 *Journal of Sound and Vibration*, **192,** 821–833. Quasi-periodic response and stability analysis for nonlinear systems: a general approach.
9. S.-K. Choi and S. T. Noah 1992 *Nonlinear Dynamics* **3**, 105–121. Response and stability analysis of piecewise-linear oscillators under multi-forcing frequencies.
10. K. S. Kundert, G. B. Sorkin and A. S. Vincentelli 1988 *IEEE Transactions on Microwave Theory and Techniques* **36**, 366–378. Applying harmonic balance method to almost-periodic circuits.
11. D. W. Childs 1984 *Turbomachinery Report FD*-1-84. Rotordynamic characteristics of the HPOTP of the SSME.
12. J. M. Vance 1988 *Rotordynamics of Turbomachineries*. New York: John Wiley.
13. Y. B. Kim and S. T. Noah 1991 *Nonlinear Dynamics* **1**, 221–241. Bifurcation analysis for a modified Jeffcott rotor with a bearing clearance.
14. Y. Ishida, T. Ikeda, T. Yamamoto and M. Hiei 1988 *Bulletin of the Japan Society of Mechanical Engineers* **29**, 200–207. Internal resonance in a rotating shaft system.